Water Science & Technology

Water Science & Technology Vol 85 No 4, 1065 doi: 10.2166/wst.2022.035

Enhanced sequestration of molybdenum(VI) using composite constructed wetlands and responses of microbial communities

B. Chen[a,b], F. J. Zhou[b], F. Yang[c], J. J. Lian[a,b], T. R. Ye[b], H. Y. Wu[b], L. M. Wang[c], N. Song[d,*], Y. Y. Liu[b] and A. Y. Hui[b]

[a] Key Laboratory of Metallurgical Emission Reduction & Resources Recycling (Anhui University of Technology), Ministry of Education, Ma'anshan 243002, China
[b] College of Energy and Environment, Anhui University of Technology, Anhui 243002, China
[c] Nanjing Institute of Environmental Sciences, Ministry of Ecology and Environment, Nanjing 210042, China
[d] College of Marine Science and Engineering, Nanjing Normal University, Nanjing 210023, China
*Corresponding author. E-mail: nsong@niglas.ac.cn

FY, 0000-0003-3326-9615

ABSTRACT

The molybdenum (Mo) non-point source pollution in the mining area has an irreversible impact on the surrounding water and soil ecosystems. Herein, three integrated vertical subsurface flow constructed wetlands (CWs) were constructed to assess the effects of combination substrates and plant on the removal of Mo(VI). Results showed that CW1 with combination substrates and cattail exhibited a favorable removal performance for Mo(VI) at 80.90%. Moreover, most Mo(VI) retained in the CWs was retained in the substrate (58.13–88.04%), and the largest fraction of Mo(VI) retained was the water-soluble fraction on the surface of the combination substrates. Mo(VI) removal was also influenced by the microbial community composition in substrate, especially their co-occurrence networks. The species that showed significant positive correlation with Mo(VI) removal were Planctomycetes, Latescibacteria, Armatimonadetes, and Gemmatimonadetes. Moreover, CWs added plants showed that more co-occurrences interaction between taxa occurs, which means that the wetlands efficiently select recruitment of potential microbial consortia and change the co-occurrences to remove pollution in the substrate. These results could be useful in providing an ecology-based solution for the treatment of Mo(VI) in wastewater, especially in adjusting the microbial communities for Mo(VI) removal at the genetic level.

Key words: adsorption mechanism, constructed wetlands, drinking water treatment residuals, molybdenum removal, response relation

HIGHLIGHTS

- Complex substrates coupled cattail enhanced Mo(VI) removal in constructed wetlands.
- Adsorption was the main Mo(VI) removal mechanism by DWTRs and MCPP.
- Mo(VI) removal was also influenced by microbial community composition.
- Cattails changed the co-occurrences of microbes to remove pollution in substrates.

GRAPHICAL ABSTRACT

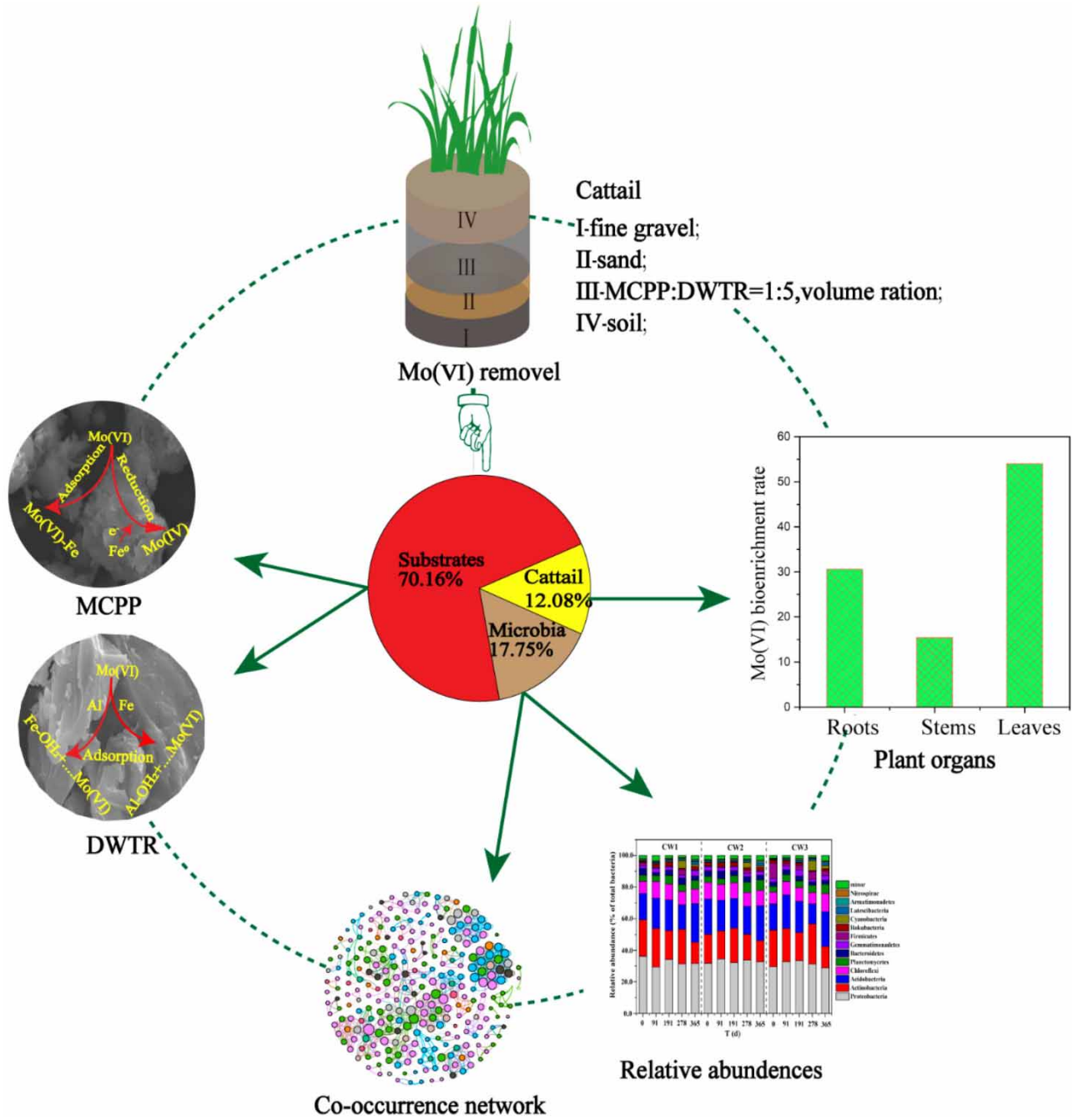

INTRODUCTION

Molybdenum (Mo) is not only a key micronutrient for both animals and plants, but it is also widely applied in industries as a component of fertilizer, catalysts, and anti-corrosive agents (Afkhami & Norooz 2009). Meanwhile, Mo also plays an important role in the function of enzymes which can reduce atmospheric nitrogen (N_2) to ammonia (NH_3) or its derivatives (Afkhami & Norooz 2009). However, due to anthropogenic activities, a large quantity of Mo-containing waste has been discharged directly into aquatic environments, leading to high contamination of Mo (>mg/L) in groundwater, rivers, lakes, and seas. The extensive exploitation of Mo in the last century has resulted in serious Mo pollution events in the Brenda Mines of

Canada (Aube & Stroiazzo 2000), and the Wujintang Reservoir, China (Yu *et al.* 2011). Mo usually exists in various valence states ranging from +2 to +6 in water solution; however, molybdate ions (MoO_4^{2-}), as the most soluble elements, are widely distributed in natural environments and in wastewater (Dong *et al.* 2014). An elevated environmental level and/or uptake of Mo(VI) can potentially cause adverse effects on human health, and result in growth retardation, sterility, hypothyroidism, anemia, and death (Lian *et al.* 2021). Thus, removal of Mo(VI) from wastewater is of significant importance in terms of an environmental point of view.

Traditional methods, such as ion exchange, reverse osmosis and advanced oxidation, have been developed for Mo(VI) removal in wastewater (Lian *et al.* 2013a). However, due to the high energy consumption, generation of the toxic sludge, as well as the high cost, ecological treatment methods seem to have more advantages. Constructed wetlands (CWs), also known as wastewater treatment wetlands, are designed to treat wastewater mainly through substrate adsorption, plant uptake, and biodegradation (Lu *et al.* 2021). Over the last few decades, CWs have been widely used for degrading nutrients and organic substances from municipal sewage and agricultural runoff (Wu *et al.* 2015), as well as for removing mine wastewater due to their economic and ecological advantages. Many wetlands have been constructed to naturally treat wastewaters polluted by abandoned acid mine drainage (Vymazal & Brezinova 2016); however, little work to date has reported using CWs to treat wastewater from alkaline mines, for example Mo tailings (Lian *et al.* 2013b).

The CW is a unique integrated ecosystem of substrates, plants and microorganisms. The substrate layer including substrates and microorganisms in CWs plays a vital role in the treatment of heavy metal wastewater. Especially, iron as the substrate plays an important role in the removal of phosphorous, sulfur, and metals in all kinds of CWs (Wu *et al.* 2019). As a by-product of the treatment process in the water purification plant, drinking water treatment residues (DWTRs) have received increasing attention from wastewater management officials and other scientists specializing in ecological remediation (Wang *et al.* 2021). Previous studies have shown that DWTRs have a strong adsorption potential for phosphorus due to its highly reactive surface and relatively high amounts of Al and Fe (Wang *et al.* 2021). Our recent work has suggested that DWTRs was an efficient, green and recyclable adsorbent for Mo(VI) removal by surface complexation and electrostatic interaction (Lian *et al.* 2019). Besides, biochar has been widely used as an adsorbent and soil conditioner for its high porosity and huge specific surface area, which can affect the migration and bioavailability of contaminants (Wang *et al.* 2013). Furthermore, biochar can act as an electron shuttle between Fe(III) minerals and bacteria (Kappler *et al.* 2014), as well as stimulating the related bacterial activities to enhance As(V) and Fe(III) reduction (Chen *et al.* 2016). Previous study has shown that a new modified carbonized pomelo peel biosorbent (MCPP), made from zero-valent iron and cetyl-trimethyl ammonium bromide, has a proven ability to remove Mo(VI) from wastewater (Lian *et al.* 2018). Therefore, if DWTRs and MCPP are used as composite substrates in CWs, they will not only improve the removal rate of Mo(VI) from adsorption, but they can also use their natural affinity with microbial activities to capture Mo(VI). Microbial community structure plays a key role in determining the environmental fate of heavy metals. Diaby *et al.* (2015) found that the heavy metal pollution caused by copper tailings can be effectively repaired by CWs, and the composition of the microbial community changes significantly over time. Unfortunately, to date, related studies conducted using the combined DWTRs/MCPP substrates to promote the removal of Mo(VI) in CWs has not been reported, let alone the dynamic response of microorganisms to Mo(VI) pollution.

This study constructed three different CWs to analyze their long-term effects on Mo(VI) removal and their microbial response characteristics. The specific objectives were: (1) to evaluate the long-term treatment performance of Mo(VI) by CWs based on DWTRs and MCPP; (2) to explore the speciation of Mo(VI) in the substrate and the distribution of Mo(VI) in plants; (3) to discern the dynamic response characteristics of the key microbe to Mo(VI) pollution. This study will provide guidance on the selection of substrate type and regulation of microbial to remove Mo(VI) wastewater in CWs.

MATERIAL AND METHODS

Chemicals and materials

Sodium molybdate 2-hydrate ($Na_2MoO_4{\cdot}2H_2O$) was used to prepare a Mo(VI) stock solution with a concentration of 1000 mg/L, which will be diluted with deionized water to the required concentration. All chemicals such as sodium hydroxide and hydrochloric acid were analytical grade and purchased from Sinopharm Chemical Reagent Co., Ltd (China). Pomelo peel, collected from a local market as solid waste, was washed several times with deionized water to remove the dirt particles on the surface, and then dried, ground, and pulverized to a $<$2.0 mm particle size. The MCPP was synthesized using the

method described by Lian *et al.* (2018). Briefly, the pomelo peel was carbonized at 500 °C for 1 h in a tube furnace. Thereafter, a certain amount of carbonized pomelo peel was mixed with 0.2 mol/L $FeSO_4$ aqueous solution and stirred for 1 h in an N_2 environment; then, 0.2 mol/L KBH_4 and 0.02 mol/L of cetyltrimethyl ammonium bromide (CTAB) were added to the solution in sequence and stirred for another 1 h. Finally, the prepared MCPP was dried at 60 °C in a vacuum oven for 12 h, and was stored in a sealed polyethylene container for further studies. The DWTRs were taken from the Capital water treatment plant in Maanshan City, China, which primarily treats surface water from the Changjiang River. Fresh DWTRs samples were washed, air-dried, milled and sieved (<0.2 mm) prior to use. Deionized water was used throughout the entire experiment.

Configuration of constructed wetlands microcosm

Three buckets with the following dimensions: height (26 cm), lower diameter (23 cm) and upper diameter (26 cm) were used to simulate the CWs (labeled CW1 to CW3). Details are shown in Figure 1. The volume of each empty bucket was about 10 L, and the original porosity of CW1, CW2, and CW3 was 20.3, 19.6, and 19.4%, respectively. The filling sequence of the substrates and the planting situation in three vertical-flow wetland buckets are also shown in Figure 1. Fine gravel (1–10 mm), sand (<0.5 mm) and cattail (*Typha latifolia*) were obtained from a river-bank (Jiangxinzhou sub-district, Maanshan), and the sand was washed and air-dried before use. Cattail efficiently removed Mo(VI) in our previous study (Lian *et al.* 2013b), so five rhizomes of cattail were planted in CW1 and CW3.

Wetland operational procedures

Three vertical-flow CWs were placed in an open laboratory, which were directly and indirectly exposed to daylight and artificial light. The ambient temperature range was between 12.5 and 25.7 °C throughout the experiment. Insufficient amounts of organic matter were collected from the local tailings pond. Furthermore, Fe, Zn and Cu hardly migrated in alkaline conditions prevailing in Mo tailings pond (Yu *et al.* 2011); thus, the influent was prepared with tap water containing only Mo(VI) solution. The average concentration of Mo(VI) in the influent was 5.53 mg/L, which has been found in various environments (Table S1), and the initial pH of the influent throughout the experiment was about 7.2.

To simulate the storm runoff, the system operated in an intermittent manner. First, during the plant cultivation period before being transferred to the constructed wetland, Hoagland nutrient solution without molybdenum was used. Then a

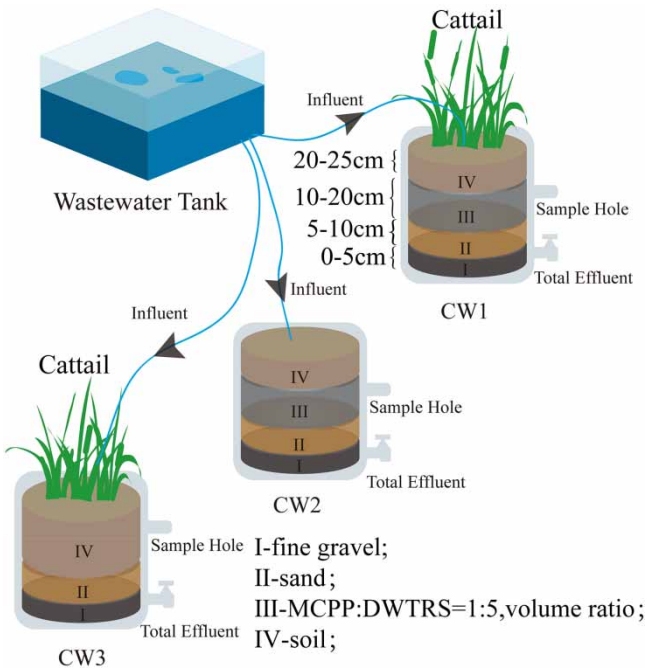

Figure 1 | Schematic diagram of laboratory-scale constructed wetland. CW1: DWTRs+MCPP+Cattail; CW2: DWTRs+MCPP; CW3: Soil+Cattail.

1-week startup period (in September 2018) was allocated to facilitate the development of plant roots. Afterwards, three devices were operated continuously for one year. A 7-day running cycle was established for every week of the experiment's year. In detail, the test started with a hydraulic retention time (HRT) of 4 days, then drained out and rested for up to 3 days. The water level of the device was lowered within 1 min until approximately 5 cm of water remained below the soil surface. The aim of this process was not to destroy the microbial distribution and form a subsurface zone. The water outlet was arranged at one side of the device bottom. In all experiments, the inflow water was never in contact with plant leaves in CW1 and CW3 to avoid Mo(VI) precipitation on leaf surfaces. A simple soapy water (glycerin, sodium tallowate and sodium chloride dissolved in deionized water) was used to prevent aphids from damaging plant leaves.

Sample analysis and instrumentation

Collected water samples from influent and outlet were analyzed every 7 days. Triplicate plant samples and substrates were collected at the end of the whole experiment. The substrate samples, collected respectively from 10 to 20 cm depths of the three devices, were air-dried and milled to pass through a 250 μm sieve. Samples for sequential metal extraction in CW1 were also analyzed following the procedures described by Fox & Doner (2003). The surface characteristics of substrates were measured using scanning electron microscopy (SEM; JSM-6490LV, Japan). Powder X-ray diffraction (XRD) patterns were recorded at an interval of 0.33° with 2θ from 10 to 80° by an UItima IV diffractometer using Cu radiation (40 kV, 40 mA) (D8ADVANCE, Bruker Co., Germany). Fourier transform infrared spectroscopy (FTIR) spectra were obtained on a Nicolet 6700 FTIR spectrophotometer (Nicolet Co., USA). Collected plant tissue samples were separated into leaf, stem and root samples, and then dried and ground to approximately 600 μm. Plant and substrate samples were digested with a 9:1 nitric/perchloric solution, and then Mo(VI) concentration was tested. The temperature (T), dissolved oxygen (DO) and pH were tested by a multiparameter water quality monitor (HQ40d, HACH, United States). Mo concentrations were determined using an atomic absorption spectrophotometer (AAS) (TAS-990, Beijing Persee Ltd, China).

DNA extraction, sequencing and microbial community analysis

Microorganism samples were obtained from substrates 15 cm deep every three months. Genomic DNA was extracted with the Power Soil DNA Kit (MoBio Laboratories Inc., Carlsbad, CA, USA). DNA concentration and quality were assessed with the Nanodrop instrument (Model 2000, NanoDrop Technologies Inc., Wilmington, DE). Bacteria-specific primer 341F and universal primer 907R were used to amplify the bacteria 16 S rRNA gene fragments in V4-V5 region (Selje *et al.* 2004). The sequence data was analyzed employing the Quantitative Insight into Microbial Ecology software (QIIME), version 1.9.0. We obtained 642,278 reads for 16S rDNA sequencing after quality filtering (parameters for 16S rDNA: maxambigs = 0, min length = 240; and phred quality threshold = 20; parameters for ITS: maxambigs = 0, min length = 200, and phred quality threshold = 20). OTUs were generated according to a 97% similarity level through UCLUST, and singletons were removed throughout this process. UCHIME was used to remove chimeras of 16S rDNA data. The taxonomic identity of bacteria phylotype was assigned using the Greengenes database (http://greengenes.lbl.gov), and the assignment method is BLAST, which used assign_taxonomy.py script with default parameters in QIIME. After removing the non-bacterial reads, 477, 204 bacterial reads were finally obtained. Redundancy analysis (RDA) was used to analyze environmental factors that had the most effect on the bacterial community structure. Sequencing data was deposited in the NCBI Sequence Read Archive (BioProject number PRJNA790725).

Network analyses

Co-occurrence networks were constructed to understand and visualize the interactions under different treatments. OTUs were selected by a relative abundance of more than 0.05% to simplify the data set. In a network, the nodes represent different OTUs and links indicates the presence of significant ($p < 0.05$) Spearman's correlation. The co-occurrence network properties including vertex number, edge number, network diameter, graph density, average degree, average path length, clustering coefficient, and modularity were calculated and visualized using Gephi. The connection relationships between different microorganisms were determined using the igraph package in R 3.6.2.

Statistical analyses

Data were analyzed using Microsoft Excel 2010, and figures were plotted using Origin 2016, version 9.3. The mean values in all treatment groups were compared using one-way analysis of variance (ANOVA) of the SPSS version 19.0.

RESULTS AND DISCUSSION

Mo(VI) removal performance of constructed wetlands

As shown in Figure 2, Mo(VI) removal averaged between 49.94 and 80.90% across the three CWs during the one-year operation period. Mo(VI) removal efficiency was higher in CW1 (80.90%) and CW2 (65.12%), which comprised the additional DWTRs/MCPP adsorption media. However, compared with CW2, the Mo(VI) removal rate in CW1 increased with time, which implied that the role of plants in wetland systems cannot be ignored. Cattail not only absorbed Mo(VI) directly, but also removed Mo(VI) by improving the surrounding environment of the root system indirectly, which in turn facilitated Mo(VI) removal by substrates. The change trends of the effluent DO and pH of CWs was similar, and both increased to a certain extent at the beginning of operation, and then gradually decreased, but the temperature showed the opposite trend (Figure S1). Besides, the effluent pH values of wetland systems with plants (CW1 and CW3) were lower than that of the plant-free wetland (CW2) throughout the experiment (Figure S1a). The lower pH values of CW1 and CW3 were mainly caused by CO_2 released by plant respiration and the protons and organic acids secreted from cattail roots during plant growth (Pedescoll *et al.* 2015). The adsorption efficiency of Mo(VI) by MCPP (Lian *et al.* 2018) and DWTRs (Lian *et al.* 2019) has been proven to be dependent on pH values, and low pH was beneficial to Mo(VI) removal. Therefore, lower pH values caused by plants in CW1 facilitated the removal of Mo(VI) by substrates.

As shown in Table 1, substrates were the main factor for Mo(VI) removal, which contributed about 58.13–88.04% of the Mo(VI) removal in the three CWs. The high Mo(VI) removal rate by substrate was mainly due to the existence of DWTRs and MCPP in the substrate. This phenomenon was more obvious when comparing Mo(VI) removal by sand and soil, which was low as noted in our previous studies (Lian *et al.* 2013b). DWTRs and MCPP have been proven to be sustainable, efficient, and recyclable adsorbents for Mo(VI) removal (Lian *et al.* 2018, 2019). The small Mo(VI) removal rate by cattail may be caused by the smaller wetland model, which has an adverse effect on their growth. To further investigate the distribution of Mo(VI) in cattail, Mo(VI) concentrations in all cattails of CW1 and CW3 were estimated through a series of processing, such as harvested, dried and weighed. The results indicated that the bioenrichment of Mo(VI) in leaves had the highest content (254.02 mg/kg) followed by roots (143.94 mg/kg) > stems (72.53 mg/kg), and this facilitated the complete removal of Mo(VI) from the CWs. However, the migration ability of plant roots to heavy metals is different. Some studies have shown meager migration of heavy metals by roots due to sequestration in the vacuoles of roots (Xin *et al.* 2020). This sequestration provides a natural protection of the surrounding soil, sand, and aquatic environment as it prevents the potential toxic effects of the absorbed metals (Vymazal & Brezinova 2016). The different accumulation of heavy metals by plant roots may be related to the rhizosphere microenvironment and the metal types. The proportion of Mo(VI) removed by microorganisms is calculated by subtracting the removal rate of substrates and plants from the total removal rate. Results found that more

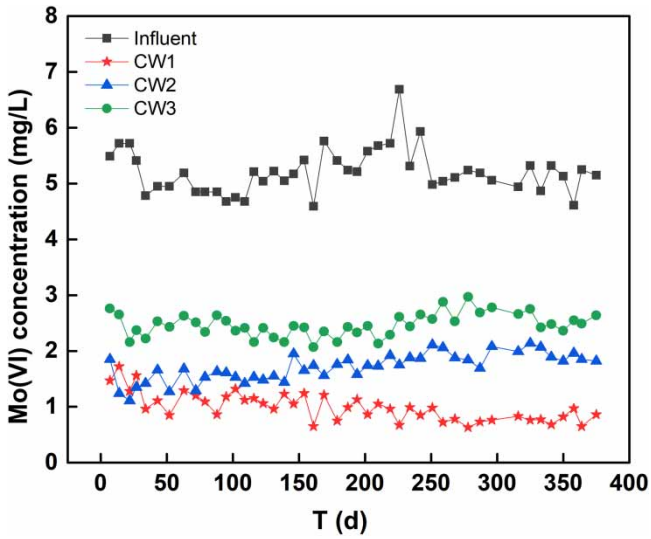

Figure 2 | Mo(VI) concentrations in influent and effluent from three CWs. CW1: DWTRs + MCPP + Cattail; CW2: DWTRs + MCPP; CW3: Soil + Cattail.

Table 1 | The percentage of Mo(VI) removed by various methods in the total removal of the CWs

	CW1		CW2		CW3	
	Mo(VI) (mg)	Removal rate (%)	Mo(VI) (mg)	Removal rate (%)	Mo(VI) (mg)	Removal rate (%)
In	468.62 ± 4.73[a]		440.19 ± 6.95		443.77 ± 4.09	
Out	89.5 ± 3.85	80.90	153.52 ± 3.03	65.12	222.14 ± 4.65	49.94
Substrate[b]	266.04 ± 7.96	70.16	252.38 ± 9.53	88.04	128.84 ± 7.58	58.13
Vegatative biomass[c]	45.8 ± 6.94	12.08	0	0	55.48 ± 8.79	25.03
Microbial processing[d]	67.28	17.75	34.29	11.96	37.31	16.83
Total removal	379.12		286.67		221.63	

[a]Data presented as mean ± standard deviation.
[b]A mixture of MCPP and DWTRs (10–20 cm).
[c]Sum of all cattail in each system including roots, stems and leaves.
[d]The value was calculated by subtracting the proportion of substrate adsorption and vegetative uptake from the total Mo(VI) removal. CW1: DWTRs + MCPP + Cattail, CW2: DWTRs + MCPP, CW3: Soil + Cattail.

Mo(VI) was removed in CW1 and CW3 treatments. It meant that plants in wetland systems may change the microbial community structure in CWs. The details will be discussed below.

Adsorption mechanism of Mo(VI) on DWTRs and MCPP

SEM-EDS analysis

As shown in Figure 3(a) and 3(c), the morphology of the raw DWTRs and MCPP samples were porous because of their intrinsic natures. After reacting with Mo(VI), pore structures of DWTRs-Mo(VI) and MCPP-Mo(VI) were relatively smaller for injection of Mo(VI) (Figure 3(b) and 3(d)). Furthermore, the rough surface of DWTRs-Mo(VI) and MCPP-Mo(VI) samples may also be caused by the microbiological corrosion, which was reported in the study of Mo(VI) removal by FeS_2 in CW systems (Lian *et al.* 2013b). The energy dispersive spectrometry (EDS) images of DWTRs (Figure S2a) illustrate that the main constituent elements are O, Al, Si, and Fe. Besides, the EDS image of Mo-spiked DWTRs showed an Mo peak in addition to the above elements (Figure S2b). Similarly, the initial MCPP mainly contained O, Mg, P, Cl, and Ca (Figure S2c). After one year of operation, an Mo peak appeared on the surface of MCPP-Mo (Figure S2d). The results show that Mo adhered to the surface of the two substrates.

XRD analysis

The XRD patterns of the DWTRs and DWTRs-Mo showed that they were mainly short-range-ordered materials due to the lack of distinct diffraction characteristic peaks (Figure 4(a)). In addition, some obvious peaks matched well with the standard SiO_2 (CSD#88) in the XRD patterns of DWTRs and DWTRs-Mo, which is also considered a typical crystal plane of DWTRs (Lian *et al.* 2019). According to the indexed XRD pattern (JCPDS No. 50-1619), the weak peaks around 19.5 °C on DWTRs-Mo belongs to $Fe_2(MoO_4)_3$. The slight difference of this peak before and after the reaction may be caused by the addition of Mo(VI). Figure 4(b) shows that diffraction peaks appearing at 25° on carbonized pomelo peel (CPP) is the characteristic peak of a graphite crystal. Characteristic peaks at 44.67° confirmed the presence of Fe^0 on MCPP compared to peaks on standard materials. Peaks of 25.5° on MCPP-Mo demonstrated the existence of MoO_2 (Sun *et al.* 2011). Intense peaks corresponding to the 2θ values of 19.5°, 20.3°, 21.7°, and 22.9° confirmed the existence of $Fe_2(MoO_4)_3$ on MCPP-Mo. These results indicated that Mo(VI) was adsorbed on MCPP partially, and the other part was reduced to a lower valence state by Fe^0.

FTIR analysis

The active bonds and groups on the surface of materials have a certain influence on the adsorption performance of metals onto materials. The spectra of DWTRs and MCPP before and after Mo(VI) reaction is shown in Figure 4(c) and 4(d). The peaks around 3444 and 3421 cm^{-1} were assigned to stretching vibration of O-H and –NH groups (Lou *et al.* 2015). The peaks at 1643 and 1614 cm^{-1} were assigned to the carboxyl function group (-COO^-) (Iqbal *et al.* 2009). The bands between 500 and 800 cm^{-1} were assigned to the stretching vibrations of the Al-O nucleus (Mohapatra *et al.* 2009), and their change is related to the intervention of Mo(VI), such as Mo = O stretching (Shan *et al.* 2016). The modification of the peak at 1037 cm^{-1}, which was attributed to the hydroxyl vibrations of iron oxyhydroxides (Namduri & Nasrazadani 2008), indicates

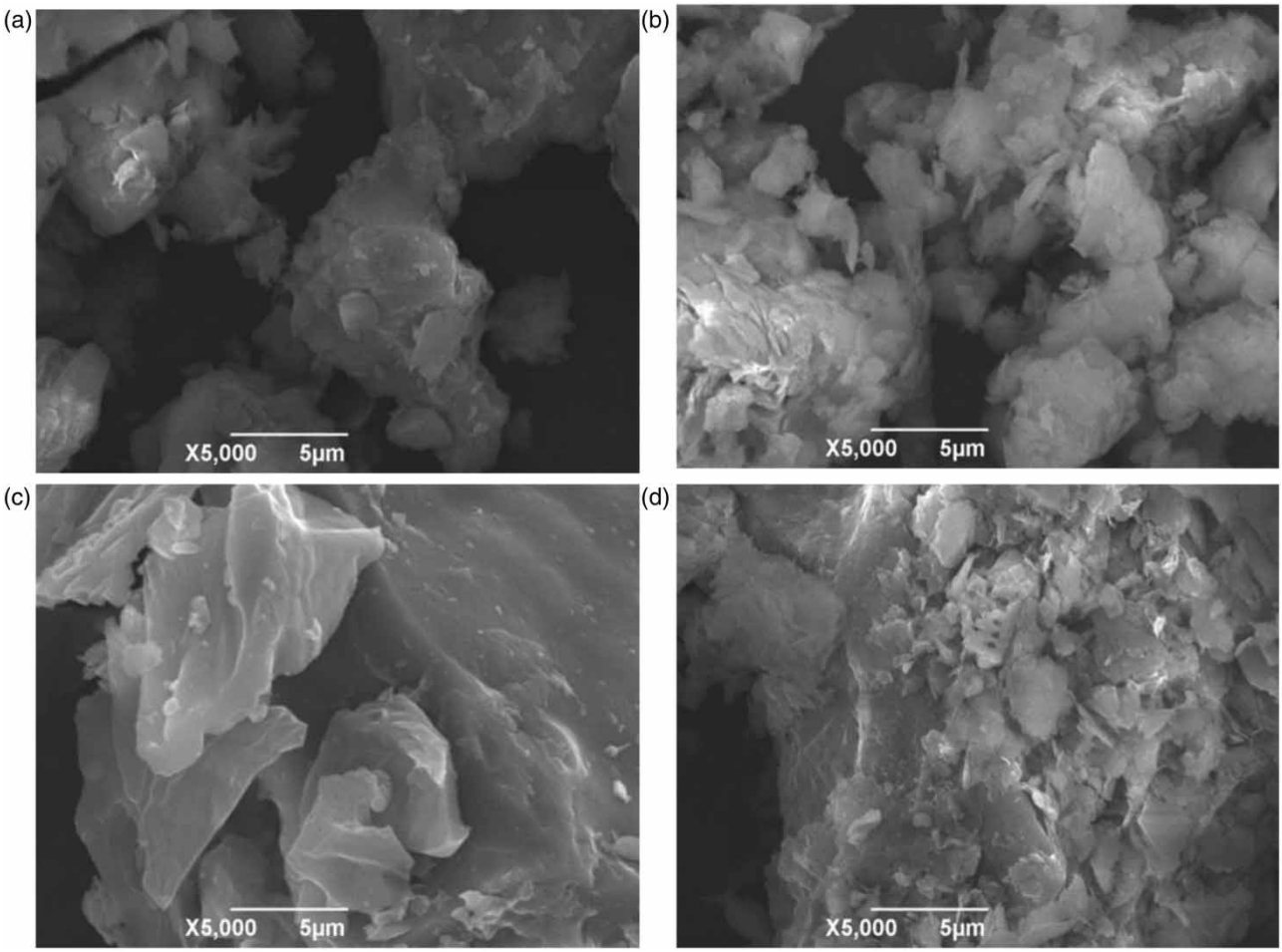

Figure 3 | SEM analysis of DWTRs (a), DWTRs-Mo(VI) (b), MCPP (c), and MCPP- Mo(VI) (d).

that M = O (M: V, Mo, and W) represent a stretching of coordinatively unsaturated surface Mo^{n+} ions, which can coordinate with Fe ions. The above changes indicate that the metallic oxides on the surface of absorbents interacts with Mo(VI), which is similar to the Mo(VI) adsorption by desulfurized steel slag and cinders (Lian *et al.* 2013a).

Speciation of Mo(VI) in the substrate

The speciation patterns of Mo(VI) on the composite substrate are important to gain a greater understanding of the fate of Mo in the constructed wetland. As shown in Table 2, most of the accumulation of Mo(VI) in CW1 occurred in the water-soluble fraction. This indicated that the removal of Mo(VI) by CW1 was mainly accomplished by ion complexation or ion exchange, which was consistent with the characterization results of Mo(VI) removal by the two substrates. This was also similar to the results of Fox & Doner (2003), who found that the majority of Mo(VI) was present in water-soluble fraction in mineral and soil obtained from a wetland. The speciation of Mo(VI) on the surface of DWTRs was retained in less stable forms (acid residue) than that of MCPP, which may be caused by the partial reduction of Mo(VI) to MoO_2 by MCPP. The result implied that molybdenum could be better utilized by plants and microorganisms, and a higher Mo(VI) removal from water can be obtained.

Microbial communities in CW systems

Microbial diversity and composition

The Shannon and Chao1 values suggested that the bacterial diversity were higher in CW2 compared to CW1 and CW3 (Figure 5(a) and 5(b)). To clarify the differences between bacterial phylogenetic groups with the samples, we investigated the relative abundance of the microbial community composition at the phylum level in each of the three CWs (Figure 5(c)).

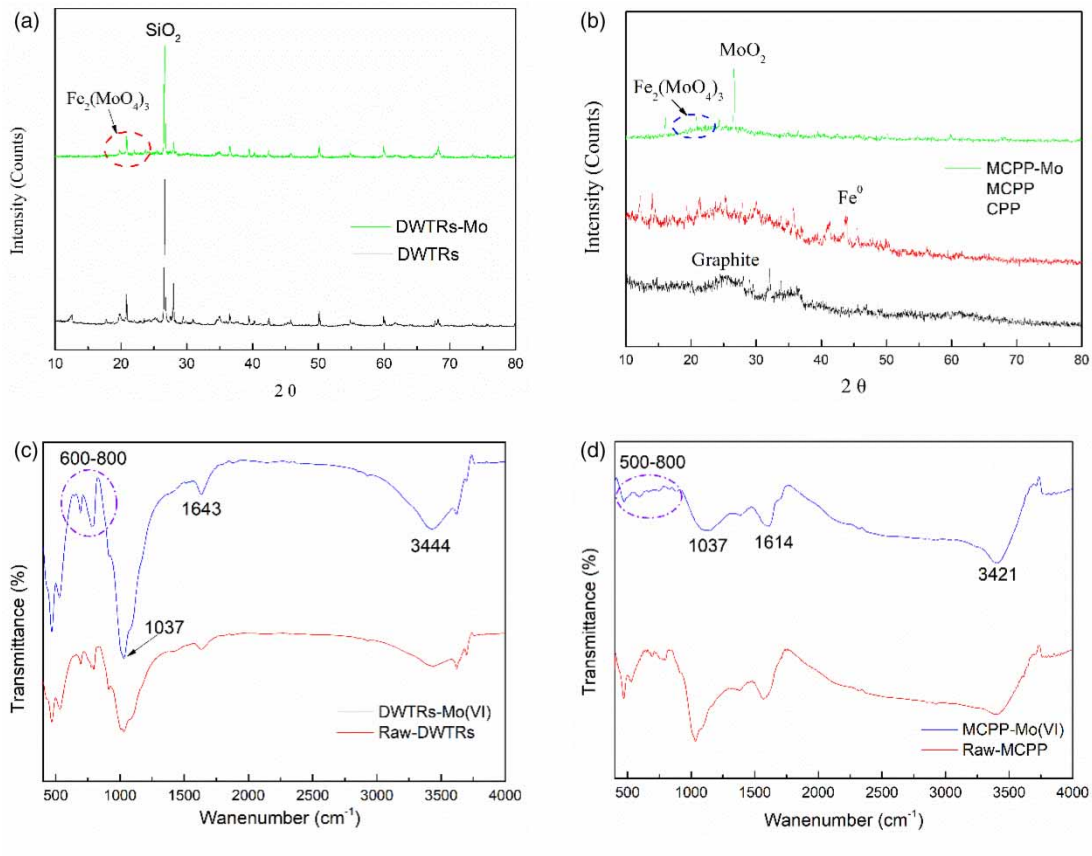

Figure 4 | XRD patterns and FTIR spectra of DWTRs (a, c) and MCPP (b, d) before and after Mo(VI) reaction.

Table 2 | Speciation proportion of Mo(VI) (%) on the two substrates in CW1

Substrate type	Water Mo(VI)	Phosphate	Acetate	NaOH	Acid
DWTRs	70.42 ± 5.43[a]	12.94 ± 1.50	9.09 ± 2.96	11.87 ± 2.88	3.88 ± 0.41
MCPP	64.55 ± 6.58	10.89 ± 1.22	7.33 ± 0.85	15.60 ± 1.73	5.72 ± 0.62

[a]Data presented as mean ± standard deviation.

The results indicate that the microbial community composition of the three CWs was not significantly different. *Proteobacteria* were the majority phyla with a content ranging between 28.7 and 36.2% in the three CWs, whereas *Actinobacteria* had a 13.3–25.4% content, *Acidobacteria* accounted for 12.6–24.5%, and *Chloroflexi* made up 7.2–11.3%. *Proteobacteria* are widespread in metal reduction environments, and they also play a key role in arsenic (As) and iron (Fe) mobilization (Dong *et al.* 2014). Compared with the initial microbial composition in the original sample, the relative abundance of *Proteobacteria* and *Actinobacteria* decreased at 365 d, while *Acidobacteria* increased. *Actinobacteria* is suitable for survival under reducing conditions, therefore the relative abundance of *Actinobacteria* decreased for the increase of DO concentration at 365 d (Figure S1b). The relative abundance of *Acidobacteria* increased at 365 d and may be related to the acidic condition and mineral iron-rich environments, which was also reported by Dedysh & Damste (2018). Compared with CW2, the pH values of CW1 and CW3 were less than 7.0 on the 365th day, so the increase of the relative abundance of *Acidobacteria* in CW1 and CW3 was more obvious than that in CW2.

The dominant genera (i.e. >2% of the total sequences in each sample) in different samples were analyzed to further illustrate the impact of Mo(VI) on bacteria (Figure 5(d)). Obviously, some differences exist between the main genera of the composite substrate layer and the soil, especially the *Bacillus* genus, which can colonize various habitats ranging from

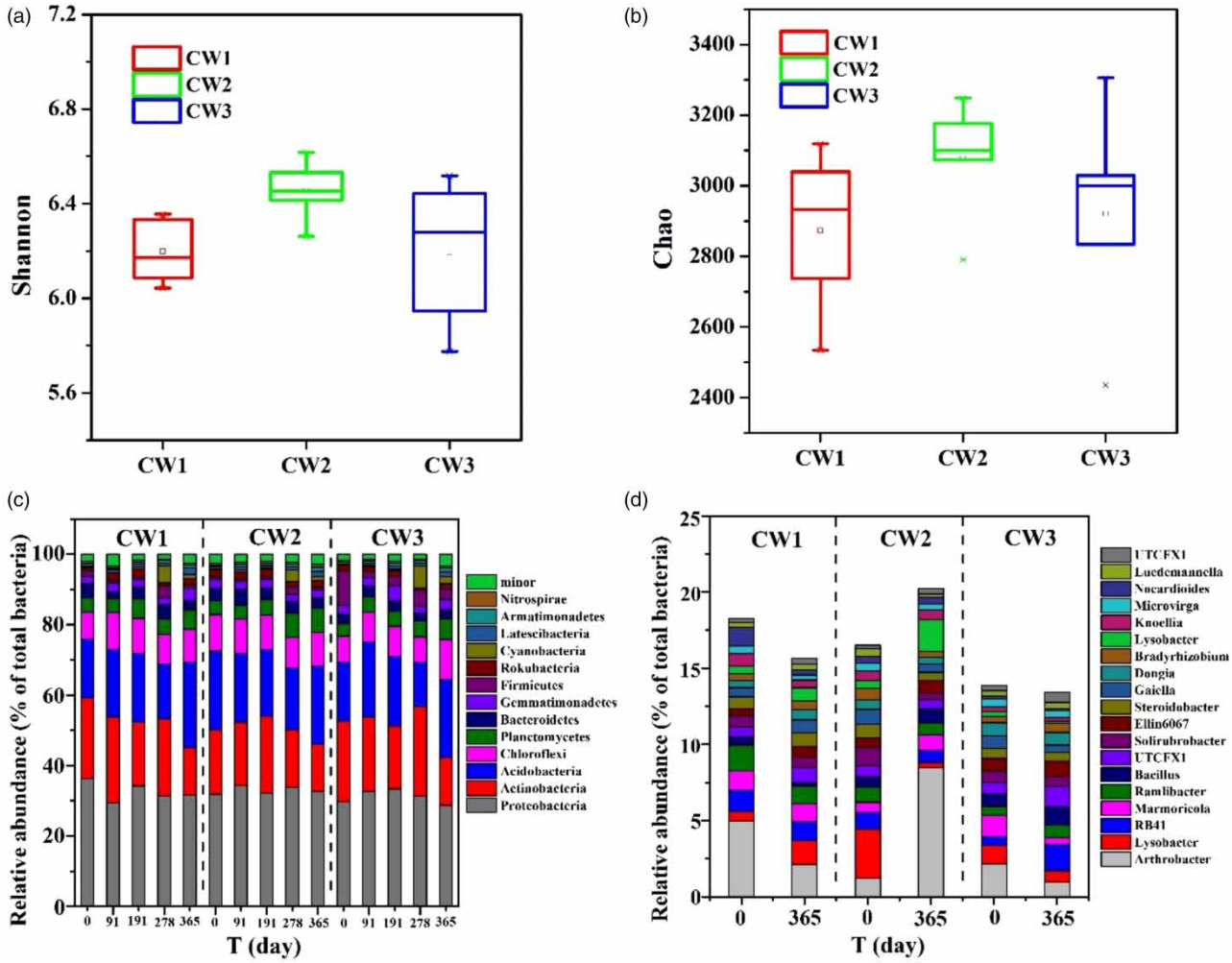

Figure 5 | Shannon and Chao values of three types of CWs (a and b). Relative abundances of bacterial phylogenetic groups at the phylum and genus level in different substrates sampled on days 0, 91, 191, 278, and 365 of the experiment (c and d). CW1: DWTRs + MCPP + Cattail; CW2: DWTRs + MCPP; CW3: Soil + Cattail.

soil to insects (Kunst 1997). *Arthrobacter* are the basic soil bacteria; they genetically branch from the Gram-positive phylum Actinobacteria. Moreover, many species of this genus dominate the soil microflora of different plants and participate in the biosorption of toxic metals (including copper (Cu), manganese (Mn), lead (Pb) and chromium (Cr)) (Megharaj *et al.* 2003). *Lysobacter* members of the phylum *Proteobacteria* are aerobic (Islam *et al.* 2005). Compared with the original samples, the relative abundance of the above two genera decreased on the 365th day. This may be due to the fact that these two bacteria are both alkalophilic and aerobic bacteria. Therefore, since the pH and DO of the system decrease in the late stage of system operation, the system environment is not conducive to the survival of these two bacteria.

Co-occurrence networks

To compare the co-occurrence patterns under different treatments (CW1, CW2, and CW3), network analysis was conducted based on the robustness of the co-occurrence scores (Figure 6). Positive correlations accounted for more than half of the total correlations in all three networks, especially in CW1 and CW3 networks. Topological properties (Table 3) were calculated to describe the difference of co-occurrence patterns among samples. Results revealed that all the networks were clustered, modular, and formed a small world topology. An interesting phenomenon also found was that although the microbial community composition in CWs did not change significantly, the co-occurrence patterns showed obvious differences, expecially in CW1 and CW3. The values of Vertex number, edge number, cluster coefficient, and modular were higher in CW1 and CW3 networks compared to CW2. We concluded that there were more co-occurrences in the treatments. Considering the higher

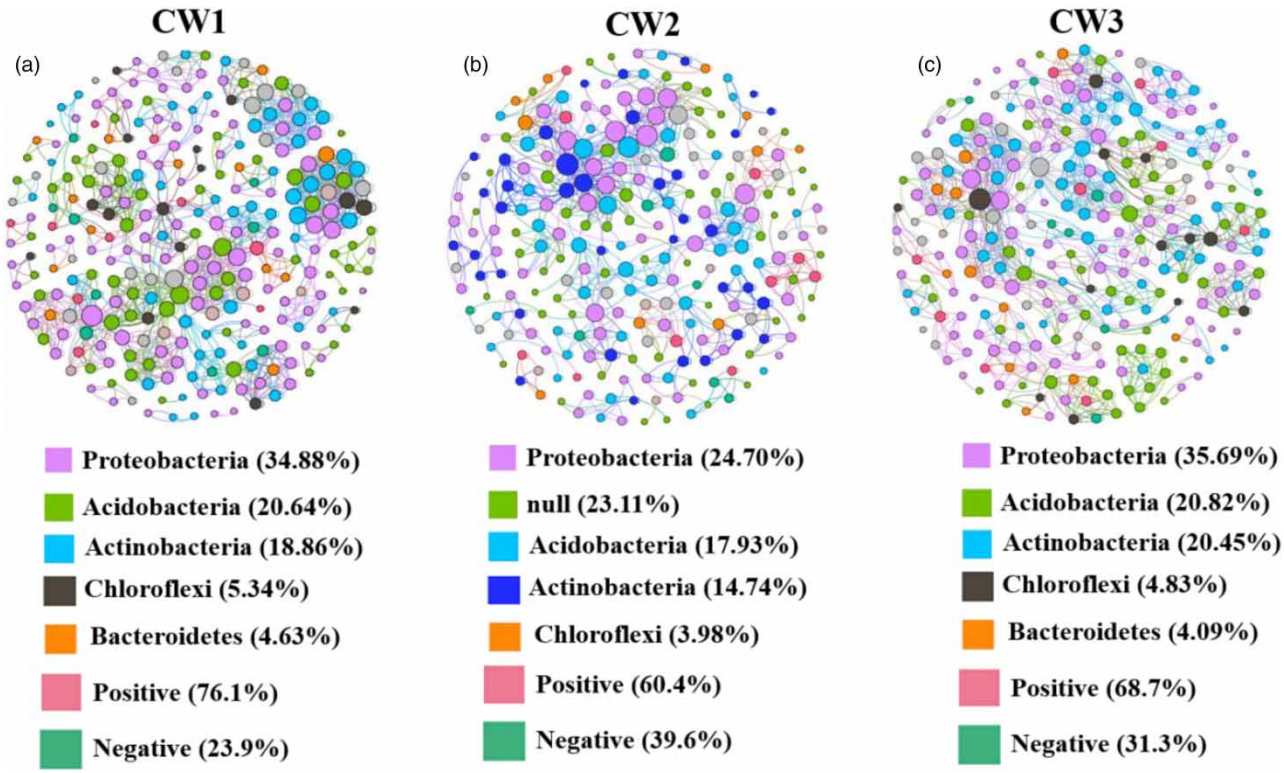

Figure 6 | The co-occurrence network interactions of bacterial community at the phylum level in the three types of CWs. The size of each node is proportional to the number of connections (i.e. degree). OTUs colored by phylum.

Table 3 | The topological properties for co-occurrence networks of the samples collected from different treatments

	Samples		
Topological property	**CW1**	**CW2**	**CW3**
Vertex number	281	194	269
Edge number	1,418	876	1,296
Diameter	14	14	9
Density	0.036	0.028	0.036
Average degree	5.494	6.98	9.628
Average path length	4.037	4.284	3.933
Cluster coefficient	0.934	0.843	0.898
Modular	2.365	1.389	1.548

removal rate of Mo(VI) by microorganisms in added plant groups (CW1 and CW3), we speculate that plant root exudations and secondary metabolites efficiently select the recruitment of potential microbial consortia and change the co-occurrences to remove pollution in the substrate (Xin *et al.* 2020).

Key functional bacteria for Mo(VI) removal

RDA was performed to identify correlations among changes in the microbial community and the different treatments during the experiments (Figure 7). Results determined that *Planctomycetes*, *Latescibacteria*, *Armatimonadetes*, and *Gemmatimonadetes* were the most relative microbes in the three CWs at the end of the experiment. Most *Planctomycetes* are mesophiles in pure culture, but some thermophile species also exist (Fuerst 2017). Figure S1c clearly shows that the temperatures of the three CWs are higher in the middle and late stages, so the relative abundance of *Planctomycetes* in this period is higher.

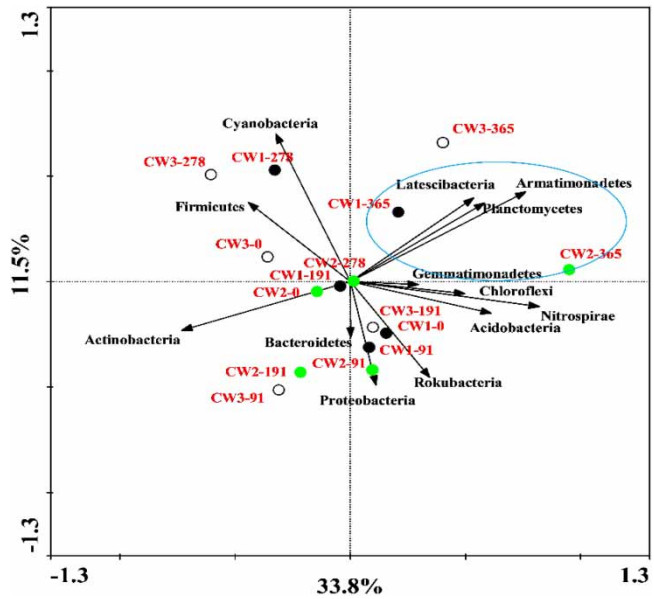

Figure 7 | Redundancy analysis (RDA) of the links of the bacterial community and the different treatments. The black circles represent the CW1 treatment samples. The green dots represent the CW2 treatment samples. The black dots represent the CW3 treatment samples.

Many *Planctomycetes* undergo 'anammox' metabolism, a process in which ammonia is directly oxidized to nitrogen by nitrate (Ward-Rainey *et al.* 1996). Moreover, note that the emergence of Cyanobacteria closely relates to molybdenum nitrogenases (Schrautemeier *et al.* 1995), which suggests that molybdenum may participate in the soil nitrogen cycle. Nevertheless, whether *Planctomycetes* affected Mo(VI) removal or not in the process of participating in the nitrogen cycle, it is still worth further exploration. The phylum *Armatimonadetes* are widespread in various terrestrial and aquatic environments, including temperate soils and wastewater treatment plans (Lee *et al.* 2014). Notably, the phylum *Armatimonadetes* has three characteristics: various preferred habitats, relatively high abundance, and properties that make it difficult for researchers seeking to obtain a pure culture. It is reported that the phylum *Latescibacteria* has a significant ability to degrade proteins and polysaccharides predominant in plant, bacteria and fungi (Farag *et al.* 2017). The above two bacteria have also played a key role in Mo(VI) removal by CWs. However, there are relatively few studies on these two bacteria. The interaction between the two bacteria and Mo(VI) removal in CWs needs further exploration.

Implications

It is well known that the substrates play a key role in the removal of heavy metals from wastewater in CWs. However, at present, the type of substrates used in most CWs is relatively simple, i.e. sand, gravel, limestone (Ji *et al.* 2022), and cinder (Lian *et al.* 2013b). How to select composite substrates and maximize the long-term removal ability of CWs has become a key remediation factor. In addition, the effect of the composite substrates on the response characteristics of the microbial community structure in CWs is unclear, which is crucial for the long-term removal of CWs.

We found that CW1 containing DWTRs, MCPP, and cattail had a higher and more stable Mo(VI) removal rate, and that this combination of substrates was the main factor for Mo(VI) removal. Notably, Mo(VI) was mainly removed by DWTRs and MCPP through adsorption and was partially reduced to a lower valence state by MCPP, which was consistent with our previous researches (Lian *et al.* 2018; Lian *et al.* 2019). We did not compare Mo(VI) removal rates to CWs composed of a single DWTRs or MCPP substrate, which were significantly improved compared with previously CWs (24.7%) composed of cinder and modified cinder (Lian *et al.* 2013b). The bioaccumulation of Mo(VI) in cattails was noted in their leaves, roots and stems. This indicates that Mo(VI) can be completely removed by harvesting the aboveground parts of plants in a CW; furthermore, this information provides an important reference value for phytoremediation of Mo(VI) in water or soil. The types of substrates and plants in the CWs also have an effect on the microbial composition on phylum level and co-occurrences. This will help the research community and bioremediation professionals to obtain a better understanding of migration and the transformation of Mo(VI) in CWs.

CONCLUSIONS

The enhanced CWs with the combined substrates of DWTRs and MCPP was proven feasible for Mo(VI) removal from wastewater. The proportion of Mo(VI) removal by the compound substrates was much higher than that of plants and microorganisms. The adsorption was the main removal mechanism for Mo(VI) by two substrates and microbes in the substrate also played an important role for Mo(VI) remove. The relative abundance and composition of microbes in the substrate layer of CWs was not significantly different on phylum lever, but showed obvious differences on genus level. *Proteobacteria* occupied the majority (28.7–36.2%) in three CWs, and *Planctomycetes*, *Latescibacteria*, *Armatimonadetes*, and *Gemmatimonadetes* were the most relative microbes to CWs remediation at the end of the experiments. However, the identification of molybdenum-resistant bacteria and the process of molybdenum removal are still unclear. Therefore, future research is needed to designate the key gene of molybdenum resistance and the influence of other environmental factors such as organic matter and inorganic ions.

ACKNOWLEDGEMENTS

This research was supported by the National Natural Science Foundation of China (51709001, 51879256, 41807464), Key Laboratory of Metallurgical Emission Reduction & Resources Recycling (Anhui University of Technology) (JKF21-05), Key R&D Program of Ningxia Hui Autonomous Region (Special Project for S&T Cooperation with unit outside the province in 2019) (2019BFG02028), and the National College Student Innovation and Entrepreneurship Training Program of Anhui University of Technology (202110360132).

DATA AVAILABILITY STATEMENT

All relevant data are included in the paper or its Supplementary Information.

REFERENCES

Afkhami, A. & Norooz, A. R. 2009 Removal, preconcentration and determination of Mo(VI) from water and wastewater samples using maghemite nanoparticles. *Colloids and Surfaces A: Physicochemical and Engineering Aspects* **346**, 52–57.

Aube, B. C. & Stroiazzo, J. 2000 Molybdate treatment at Brenda mines. In: *Proceedings of the 5th International Conference of Acid Rock Drainage*. ICARD 2000, Vols. I and II, Englewood, CO, Society for Mining, Metallurgy & Exploration, pp. 1113.

Chen, Z., Wang, Y. P., Xia, D., Jiang, X. L., Fu, D., Shen, L., Wang, H. T. & Li, Q. B. 2016 Enhanced bioreduction of iron and arsenic in sediment by biochar amendment influencing microbial community composition and dissolved organic matter content and composition. *Journal of Hazardous Materials* **311**, 20–29.

Dedysh, S. & Sinninghe-Damste, J. 2018 Acidobacteria. *eLS*, 1–10. https://doi.org/10.1002/9780470015902.a0027685.

Diaby, N., Dold, B., Rohrbach, E., Holliger, C. & Rossi, P. 2015 Temporal evolution of bacterial communities associated with the in situ wetland-based remediation of a marine shore porphyry copper tailings deposit. *Science of the Total Environment* **533**, 110–121.

Dong, G., Huang, Y., Yu, Q., Wang, Y., Wang, H., He, N. & Li, Q. 2014 Role of nanoparticles in controlling arsenic mobilization from sediments near a realgar tailing. *Environmental Science & Technology* **48** (13), 7469–7476.

Farag, I. F., Youssef, N. H. & Elshahed, M. S. 2017 Global distribution patterns and pangenomic diversity of the candidate phylum '*latescibacteria*' (WS3). *Applied and Environmental Microbiology* **83** (10), e00521.

Fox, P. M. & Doner, H. E. 2003 Accumulation, release, and solubility of arsenic, molybdenum, and vanadium in wetland sediments. *Journal of Environmental Quality* **32** (6), 2428–2435.

Fuerst, J. A. 2017 Planctomycetes – new models for microbial cells and activities. In: Kurtböke, I., (ed.). *Microbial Resources: from Functional Existence in Nature to Applications*. Academic Press, London, pp. 1–27.

Iqbal, M., Saeed, A. & Zafar, S. I. 2009 FTIR spectrophotometry, kinetics and adsorption isotherms modeling, ion exchange, and EDX analysis for understanding the mechanism of Cd^{2+} and Pb^{2+} removal by mango peel waste. *Journal of Hazardous Materials* **164** (1), 161–171.

Islam, M. T., Hashidoko, Y., Deora, A., Ito, T. & Tahara, S. 2005 Suppression of damping-off disease in host plants by the rhizoplane bacterium *Lysobacter* sp. strain SB-K88 is linked to plant colonization and antibiosis against soilborne Peronosporomycetes. *Applied and Environmental Microbiology* **71**, 3786–3796.

Ji, Z. H., Tang, W. Z. & Pei, Y. S. 2022 Constructed wetland substrates: a review on development, function mechanisms, and application in contaminants removal. *Chemosphere* **286**, 131564.

Kappler, A., Wuestner, M. L., Ruecker, A., Harter, J., Halama, M. & Behrens, S. 2014 Biochar as an electron shuttle between bacteria and Fe(III) minerals. *Environmental Science & Technology Letters* **1** (8), 339–344.

Kunst, F. 1997 The complete genome sequence of the gram-positive bacterium *Bacillus subtilis*. *Nature* **390** (6657), 249–256.

Lee, K. C. Y., Dunfield, P. F. & Stott, M. B. 2014 The phylum Armatimonadetes. In: (Rosenberg, E., DeLong, E. F., Lory, S., Stackebrandt, E. & Thompson, F., (eds)). *The Prokaryotes*. Springer, Heidelberg, pp. 447–458.

Lian, J. J., Xu, S. G., Chang, N. B., Han, C. W. & Liu, J. W. 2013a Removal of molybdenum(VI) from mine tailing effluents with the aid of loessial soil and slag waste. *Environmental Engineering Science* **30** (5), 213–220.

Lian, J. J., Xu, S. G., Zhang, Y. M. & Han, C. W. 2013b Molybdenum(VI) removal by using constructed wetlands with different filter media and plants. *Water Science and Technology* **67** (8), 1859–1866.

Lian, J. J., Huang, Y. G., Chen, B., Wang, S. S., Wang, P., Niu, S. P. & Liu, Z. L. 2018 Removal of molybdenum(VI) from aqueous solutions using nano zero-valent iron supported on biochar enhanced by cetyl-trimethyl ammonium bromide: adsorption kinetic, isotherm and mechanism studies. *Water Science and Technology* **2017** (3), 859–868.

Lian, J. J., Yang, M., Chen, B., Wang, S. S., Ye, T. R., Zheng, D. D. & Jiang, C. R. 2019 Characteristics and mechanisms of molybdenum(VI) adsorption by drinking water treatment residue. *Desalination and Water Treatment* **142**, 235–243.

Lian, J. J., Wang, H. L., He, H. P., Huang, W. L., Yang, M., Zhong, Y. & Peng, P. A. 2021 The reaction of amorphous iron sulfide with Mo(VI) under different pH conditions. *Chemosphere* **266**, 128946.

Lou, Z. N., Wang, J., Jin, X. D., Wan, L., Wang, Y., Chen, H., Shan, W. J. & Xiong, Y. 2015 Brown algae based new sorption material for fractional recovery of molybdenum and rhenium from wastewater. *Chemical Engineering Journal* **273**, 231–239.

Lu, S. Y., Zhang, Y., Liu, X. H., Xu, J. M., Liu, Y., Guo, W., Liu, X. B. & Chen, J. 2021 Effects of sulfamethoxazole on nitrogen removal and molecular ecological network in integrated vertical-flow constructed wetland. *Ecotoxicology and Environmental Safety* **219**, 112292.

Megharaj, M., Avudainayagam, S. & Naidu, R. 2003 Toxicity of hexavalent chromium and its reduction by bacteria isolated from soil contaminated with tannery waste. *Current Microbiology* **47** (1), 0051–0054.

Mohapatra, M., Rout, K., Mohapatra, B. K. & Anand, S. 2009 Sorption behavior of Pb(II) and Cd(II) on iron ore slime and characterization of metal ion loaded sorbent. *Journal of Hazardous Materials* **166** (2–3), 1506–1513.

Namduri, H. & Nasrazadani, S. 2008 Quantative analysis of iron oxides using Fourier transform infrared spectrophotometry. *Corrosion Science* **50** (9), 2493–2497.

Pedescoll, A., Sidrach-Cardona, R., Hijosa-Valsero, M. & Bécares, E. 2015 Design parameters affecting metals removal in horizontal constructed wetlands for domestic wastewater treatment. *Ecological Engineering* **80**, 92–99.

Schrautemeier, B., Beveling, U. & Schmitz, S. 1995 Distinct and differently regulated Mo-dependent nitrogen-fixing systems evolved for heterocysts and vegetative cells of *Anabaena variabilis* ATCC 29413: characterization of the *fdxH1/2* gene regions as part of the *nif1/2* gene clusters. *Molecular Microbiology* **18** (12), 357–369.

Selje, N., Simon, M. & Brinkhoff, T. 2004 A newly discovered *Roseobacter* cluster in temperate and polar oceans. *Nature* **427**, 445–448.

Shan, W. J., Shu, Y. N., Chen, H., Zhang, D. Y., Wang, W., Ru, H. Q. & Xiong, Y. 2016 The recovery of molybdenum(VI) from rhenium(VII) on amino-functionalized mesoporous materials. *Hydrometallurgy* **165**, 251–260.

Sun, Y. M., Hu, X. L., Luo, W. & Huang, Y. H. 2011 Self-assembled hierarchical MoO_2/graphene nanoarchitectures and their application as a high-performance anode material for lithium-ion batteries. *ACS Nano* **5** (9), 7100–7107.

Vymazal, J. & Brezinova, T. 2016 Accumulation of heavy metals in aboveground biomass of *Phragmites australis* in horizontal flow constructed wetlands for wastewater treatment: a review. *Chemical Engineering Journal* **290**, 232–242.

Wang, D. J., Zhang, W. & Zhou, D. M. 2013 Antagonistic effects of humic acid and iron oxyhydroxide grain-coating on biochar nanoparticle transport in saturated sand. *Environmental Science & Technology* **47** (10), 5154–5161.

Wang, C. H., Wei, Z., Liu, R., Bai, L. L., Jiang, H. L. & Yuan, N. N. 2021 The sequential dewatering and drying treatment enhanced the potential favorable effect of microbial communities in drinking water treatment residue for environmental recycling. *Chemosphere* **262**, 127930.

Ward-Rainey, N., Rainey, F. A., Wellington, E. M. & Stackebrandt, E. 1996 Physical map of the genome of the *Planctomyces limnophilus*, a representative of the phylogenetically distinct *planctomycete* lineage. *Journal of Bacteriology* **178** (7), 1908–1913.

Wu, S. B., Wallace, S., Brix, H., Kuschk, P., Kiru, W. K., Masi, F. & Dong, R. J. 2015 Treatment of industrial effluents in constructed wetlands: challenges, operational strategies and overall performance. *Environmental Pollution* **201**, 107–120.

Wu, S. B., Vymazal, J. & Brix, H. 2019 Critical review: biogeochemical networking of iron in constructed wetlands for wastewater treatment. *Environmental Science & Technology* **53**, 7930–7944.

Xin, J. P., Ma, S. S., Li, Y., Zhao, C. & Tian, R. N. 2020 *Pontederia cordata*, an ornamental aquatic macrophyte with great potential in phytoremediation of heavy-metal-contaminated wetlands. *Ecotoxicology and Environmental Safety* **203**, 111024.

Yu, C. W., Xu, S. G., Gang, M. Y., Chen, G. W. & Zhou, L. D. 2011 Molybdenum pollution and speciation in Nver River sediments impacted with Mo mining activities in western Liaoning, northeast China. *International Journal of Environmental Research* **5**, 205–212.

First received 14 October 2021; accepted in revised form 16 January 2022. Available online 2 February 2022